OnLine Journal of Biological Sciences

Research Article

In Vitro and *in Silico* Evaluation of Bioactive Compounds from *Usnea longissima* Ach. as Antimicrobial Agents

Oky Kusuma Atni[1], Erman Munir[1], Nursahara Pasaribu[1], Etti Sartina Siregar[1] and Mohd Nazre Saleh[2]

[1]Department of Biology, Faculty of Mathematics and Natural Sciences, Universitas Sumatera Utara, Medan, North Sumatera 20155, Indonesia
[2]Department of Forest Science & Biodiversity, Faculty of Forestry and Environment, University Putra Malaysia. Serdang 43400, Selangor, Malaysia

Article history
Received: March 10, 2024
Revised: November 18, 2024
Accepted: November 23, 2024

Corresponding Author:
Erman Munir
Department of Biology, Faculty of Mathematics and Natural Sciences, Universitas Sumatera Utara, Medan, North Sumatera 20155, Indonesia
Email: erman@usu.ac.id

Abstract: Lichens, formed from symbiotic association between of fungi with phototrophic organisms, generate a variety of bioactive chemicals having medicinal potential. This research aimed to examine the antibacterial characteristics of *Usnea longissima* Ach. using both in vitro and in silico methodologies. The effectiveness of lichen methanol extracts against different diseases was evaluated using the disc diffusion technique. Pathogens included gram-positive, gram-negative, and pathogenic yeast. The extracts showed significant antimicrobial activity, notably inhibiting *Propionibacterium acnes* (22.3±0.5 mm) and *Pseudomonas aeruginosa* (18.36±0.33 mm). GC-MS isolated 29 bioactive chemicals, some of which are derivatives of benzoic acid and 9-octadecenal. Lipinski's rule of five was used to provide an assessment of the drug-like properties of these substances. Molecular docking studies with 6KZZ protein, performed using Autodock Vina, revealed high binding affinities for compounds such as 1-propanone (−4.8 kcal/mol) and oxacycloheptadec-8-en-2-one (−5.1 kcal/mol), suggesting their potential as antimicrobial agents. In contrast, compounds including 9-octadecenal (−3.6 kcal/mol) and carbamic acid (−2.8 kcal/mol) showed weaker binding, indicating the need for further optimization. The findings underscore the need for more study into *U. longissima* as a possible source of new antibiotic compounds.

Keywords: Antimicrobial, Bioactive Compound, DNA Gyrase; Lichens, Molecular Docking

Introduction

Lichens are formed by the symbiotic interactions that exist between mycobionts, which are fungus, and photosynthetic algae and/or cyanobacteria. Over 30,000 species of lichens have been identified, contributing to 20% of the known fungal biodiversity. These species inhabit the most severe habitats on Earth. Most of the organic nutrients that are created by lichens are absorbed by mycobionts, except for a minor portion that is used for the growth and development of photobionts at the same time. Obtaining inorganic salts and moisture from the surrounding environment is accomplished by the photobiont via the hyphae of the mycobiont (Johansson *et al*., 2011). Algal cells are encased and encircled by fungal hyphae, which not only serve to build the structure of the lichen but also to protect the photobiont from the potentially harmful effects of the environment (Calcott *et al*., 2018). In most terrestrial ecosystems on Earth, mycobionts and photobionts have a symbiotic connection, which is one of the most effective ways for mushrooms to sustain themselves (Lücking *et al*., 2017). Both in terms of evolution and ecology, this connection is well-regulated by the two principal symbionts, as well as the amount of selectivity and specificity that exists between them in a reciprocal interaction (Yahr *et al*., 2004, 2006).

A vast array of naturally occurring compounds is synthesized by lichens, many of which are exclusive to species. compounds include depsides, depsidones, dibenzofurans, quinones, chromones, carotenoids, polysaccharides, monosaccharides, and aliphatic acids (Tatipamula *et al*., 2021; Macedo *et al*., 2021; Badiali *et al*., 2023). The water-soluble nature of these chemicals, which are often found linked to cell walls and protoplasts, allows for their extraction using boiling water (Gasulla *et*

al., 2021). They may constitute over 40% of the dry weight of lichens, with some excreted as crystals on the fungal hyphae (Ranković and Kosanić, 2021). Lichens, which consist of mycobionts and photobionts, are liable to produce a wide array of secondary metabolites. Because of this symbiosis, lichens can flourish in environments that would otherwise be inaccessible to them. Their capacity to endure hard circumstances is directly connected to the synthesis of one-of-a-kind metabolites that provide protection against environmental and biological difficulties (Kalra *et al*., 2023; Mitrović *et al*., 2011). Like many other types of autonomous fungi, algae, and advanced plants, lichens create metabolites, some of which are located within the cell and others outside. Dry nitrogen compounds (1.6–11.4%), carotenoids (1.5–24 mg/g), and polysaccharides (3–5%) are all present in lichen thalli (Yasmin and Jabin, 2024). Secondary metabolites produced by lichens often have an unpleasant taste and serve as defense compounds. These compounds not only protect lichens from external threats but also exhibit remarkable pharmacological potential, including antibacterial, antimicrobial, antiviral and antifungal activities, as well as antioxidant, anti-inflammatory, and antiproliferative effects (Bhattarai *et al*., 2013; Nguyen *et al*., 2014; Dandapat and Paul, 2019; Maulidiyah *et al*., 2021; Ozturk *et al*., 2021; Mendili *et al*., 2022).

Supercoiling stress relief with DNA gyrase, bacterial DNA replication and transcription, topoisomerase II. DNA binding and cutting are done by GyrA, whereas ATP binding and ligation are done by GyrB. (Ushiyama *et al*., 2020). Quinolone antibiotics, including fluoroquinolones derived from nalidixic acid, inhibit DNA gyrase by stabilizing the covalent gyrase–DNA complex, leading to DNA damage and bacterial cell death (McClendon *et al*., 2007). The PDB structure 6KZZ represents the DNA gyrase complex from *Escherichia coli* bound to an inhibitor and provides crucial insights into the binding interactions and mechanisms of these drugs. This structural information is essential for understanding how inhibitors affect DNA gyrase function and can aid in designing new antimicrobial agents and developing strategies to combat bacterial resistance. Despite the effectiveness of fluoroquinolones, bacterial resistance remains an important challenge, necessitating ongoing research to discover novel drugs and improve treatment strategies. Like synthetic antibiotics, lichen-derived metabolites with antimicrobial properties inhibit DNA gyrase. These results suggest that lichen chemicals may be natural alternatives to antibiotics and provide novel ways to treat resistant bacteria. This research examines *U. longissima* bioactive substances and their antibacterial properties. By focusing on how these compounds interact with bacterial proteins through in silico methods, the research seeks to predict their effectiveness as future drug candidates. The hypothesis is that *U. longissima* bioactive compounds possess significant antimicrobial properties, offering a natural solution to address bacterial resistance. Identifying key interactions and mechanisms may contribute to the development of novel therapies derived from lichen species.

Material and Methods

Lichen Extract Preparation

U. longissima Ach. was gathered in Taman Hutan Raya Bukit Barisan, Indonesia, after being rinsed and patted dry. Then, a blender was used to grind the dried algae. The powdered *U. longissima* was then macerated with 70% methanol for extraction. At room temperature, with a shaker set at 150 rpm, the extraction procedure was carried out in three 24-hour cycles. Using filter paper, the filtrate—which included the extract—was separated from the residue. Next, a thick *U. longissima* extract was produced by concentrating the *U. longissima* extract using a rotary evaporator. This was done again and again until it was finished. In the end, the dense of *U. longissima* extract was reduced to a concentration of fifty percent using dimethyl sulfoxide as the dissolving agent

Evaluation of Antimicrobial Properties

Pathogen Panel for Antimicrobial Assays

Pathogenic microorganisms, including three bacterial species representing both gram-positive and gram-negative strains and a pathogenic yeast, were used to evaluate antimicrobial activity. Three gram-positive bacteria (*Streptococcus mutans* ATCC 35668, *Propionibacterium acnes* ATCC 6919, and *Staphylococcus aureus* ATCC 6538), three gram-negative bacteria (*Salmonella enterica* serovar Typhii IPBCC b 11 669, *E. coli* ATCC 8739, and *Pseudomonas aeruginosa* ATCC 15442), and *Candida albicans* ATCC 10231.

Antibacterial Assay

The disc diffusion technique was used to assess the antibacterial efficacy of the *U. longissima* extract. After 20 mL of nutritious agar medium had solidified, it was spread out onto a Petri plate. The bacterial suspension's turbidity was adjusted to 50% of the McFarland criterion. Using a sterile cotton swab, the solution was distributed uniformly over the surface of the agar media. The lichen methanol extract, which contained 100 µL, was put on agar using discs. The positive control was chloramphenicol, whereas the negative control was dimethyl sulfoxide. For one day, the Petri plates were left to incubate at room temperature. We looked for evidence of bacterial growth inhibition in the discs' inhibitory zones.

Anticandida Assay

The disc diffusion technique was implemented to assess the anticandida efficacy of the *U. longissima*

extract. After 20 millilitres of potato dextrose agar had solidified, it was spread out onto a Petri plate. The turbidity of the Candida albicans suspensions was adjusted to meet the McFarland criteria. A sterile cotton brush was used to disperse the solution uniformly across the surface of the agar medium. The lichen methanol extract, which contained 100 µL, was used to cover the agar surface with discs. After 48 hours of room temperature incubation, the Petri dishes were removed. To determine how well the discs worked against Candida albicans, we measured the widths of the inhibition zones around them after incubation.

GC-MS Analysis

A microliter of *U. longissima* extract was then put into a gas chromatography-mass spectrometer. An analysis of the composition of volatile components was carried out using a Shimadzu GCMS-QP2010 Plus instrument that was equipped with a split-splitless injector and kept at a temperature of 250 degrees Celsius. The sample was inserted using the split method, and the detector of the mass spectrometer was set to a temperature of 280 degrees Celsius. One of the columns that was utilised was a Restek Rtx®-50, which was a Crossbond® 5% phenyl-50% methyl polysiloxane column. This column had dimensions of 30 m (extent), 0.25 mm (inner diameter), and 0.25 µm (layer thickness). A pressure of 64.1 kPa was applied to the helium that was used as the carrier gas. Beginning at 80 degrees Celsius for a length of two minutes, the oven temperature protocol continued until it reached 280 degrees Celsius for a duration of eight minutes. The system operated with a linear velocity of 36.6 cm/sec and an overall flow discharge of 4.9 mL/min, while the purge flow discharge was set at 3.0 mL/min. The column flow discharge was 0.99 mL/min, all of which contributed to the overall flow discharge. Each identified compound peak in the chromatogram had its mass spectrum matched to known compounds in the Wiley9.LIB database

Protein-Ligan Preparation

The following bioactive compounds of *U. longissima* Ach. were used, with the compound names and their respective PubChem IDs: 9-octadecenal, (z)- (5364492), carbamic acid, monoammonium salt (517232), propanedioic acid (867), butanoic acid (264), methane, sulfinyl-*bis*- (679), 2H-tetrazol-2-ethanal, 5-methyl- (535502), hexanoic acid (8892), 1,3-propanediol, 2-butyl-2-ethyl- (61038), cyclopentanol, 3-methyl- (86785), L-alanine, N-acetyl- (88064), 2-pyrrolidinone (12025), formamide, N-(2,4-dimethylphenyl)- (92363), isosorbide (12597), 1,4-benzenediol, 2,3,5-trimethyl- (12785), ethanone, 1-(3-butyloxiranyl)- (538285), undecanoic acid, 10-bromo- (17812), 4-methoxy-2-propylphenol (288671), 1-propanone, 1-(2,4,6-trihydroxyphenyl)- (3362), benzoic acid, 2,4-dihydroxy-3,5,6-trimethyl-, methyl ester (591722), benzoic acid, 2-hydroxy-4-methoxy-3,5,6-trimethyl-, methyl ester (606018), tetradecanoic acid (11005), hexadecanoic acid, methyl ester (8181), benzoic acid, 2,4-dihydroxy-6-methyl-, methyl ester (76658), hexadecanoic acid (985), 9,12-octadecadienoic acid (*Z*,*Z*)-, methyl ester (5284421), tetradecanoic acid, ethyl ester (31283), 4N-methylamino-2(1H)-pyrimidinone (14803475), oxacycloheptadec-8-en-2-one (5365703), cyclohexane, 1,4-dimethyl-2-octadecyl- (282770). Compound 4-[[8-(methylamino)-2-oxidanylidene-1~{H}-quinolin-3-yl[carbonylamino]benzoic acid9 (control) (PubChem CID: 146027003) was used as a reference control chemical to evaluate the inhibitory properties of the bioactive compounds obtained from *U. longissima*. The 2D and 3D structures of the active ingredients found in *U. longissima* and the control were acquired from the appropriate chemical databases on PubChem website. The structures were optimized for energy and transformed into the .pdb file format using Open Babel in PyRx software 0.8 Version.

Biological Activity Prediction

Substances derived from *U. longissima* were guessed at their biological activities using the Way2drug platform's Prediction of Activity Spectra for Substances algorithm. The prediction method involved obtaining the SMILES structure from the PubChem database and submitting it to the Way2drug server. The PASS Online exam uses the following factors to determine its results: The chance of biological activity is high when the Pa number is more than 0.7, poor when it is between 0.5 and 0.7, and inadequate when it is less than 0.5.

Prediction Drug-likeness

Chemicals were evaluated for their potential medicinal properties using The Five Principles of Lipinski (Ro5). The SwissADME tool was implemented to investigate all the substances for their drug-likeness. This data set includes the amount of hydrogen bond acceptors and donors, as well as the molecular weight and absorption. When a substance is administered orally, Ro5 determines how bioavailable it is.

Molecular Docking Analysis

We used Autodock Vina within PyRx 8.0.0 to perform docking analysis, treating the protein as a macromolecule and examining bioactive compounds and 4-[[8-(methylamino)-2-oxidanylidene-1~{H}-quinolin-3-yl[carbonylamino]benzoic acid9 as ligands (Ushiyama *et al*., 2020). Docking utilized specific grid parameters centered at (1.3057×1.4901×0.3121) with dimensions (36.7569×19.5379×18.1727 Å). The docking outcomes were visualized using Discovery Studio 2024.

Results

Lichen Morphology

Usnea longissima Ach. with a fruticose thallus, which is characterized by branched structures with secondary branches, has a dichotomous structure, smooth texture, and even edges. Thallus was not fully attached to the substrate, with the underside containing rhizines. The thallus length ranged from 10–53 cm and was light green. No reproductive structures were observed (**Fig. 1**). Chemical tests showed that the upper cortex reacted as K+ (yellow), C-, and KC-. This lichen is found in Bukit Barisan Forest, North Sumatra (Atni *et al*., 2024); Jayawijaya, Papua (Suharno *et al*., 2020); and West Java (Jannah *et al*., 2022). It inhabits corticolous environments, and it is typically located in open areas with full sunlight at altitudes ranging from 880 to 886 meters above sea level.

Antimicrobial Activity of U. longissima

The methanolic extract of *U. longissima* Ach. has potential efficacy against many pathogenic bacteria, as shown by the data in **Table 1**. The largest inhibition zone was observed against *P. acnes* ATCC 6919 (22.3±0.5 mm), indicating strong effects against Gram-positive bacteria (**Fig. 2**). This inhibition zone was larger than those of other Gram-positive bacteria tested, including those for *S. aureus* ATCC 6538 (17.16±0.10 mm) and *S. mutans* ATCC 35668 (18.86±0.07 mm). Methanol extract may impair gram-positive bacteria cell wall formation more than gram-negative bacteria, resulting in broad inhibition zones. For gram-negative bacteria, the extract also exhibited notable activity, with the largest inhibition zone against *P. aeruginosa* ATCC 15442 (18.36±0.33 mm), followed by those against *E. coli* ATCC 8739 (18.03±0.11 mm) and *S. enterica* serovar *Typhii* IPBCC b 11 669 (15.1±1.21 mm). The comparable inhibition zones in gram-negative bacteria suggest that the methanol extract has efficient penetration capabilities or mechanisms that affect the gram-negative cell walls and membranes, which can be challenging to penetrate because of the outer membrane structure. The methanolic extract exhibited moderate antifungal activity against C. albicans ATCC 10231, characterized by an inhibition zone of 9.43±0.57 mm. The methanolic extract had a 9.43±0.57 mm suppression zone around *C. albicans* ATCC 10231, which means it had some antifungal action. Although this value is lower than its antibacterial activity, these results suggest potential antifungal properties, although further optimization or concentration adjustments may be necessary to enhance its antifungal efficacy. These findings highlight the broad-spectrum antimicrobial potential of *U. longissima* methanol extract, particularly against gram-positive bacteria. Further investigation of active compounds and their action processes of action is required to fully understand their efficacy and potential therapeutic applications.

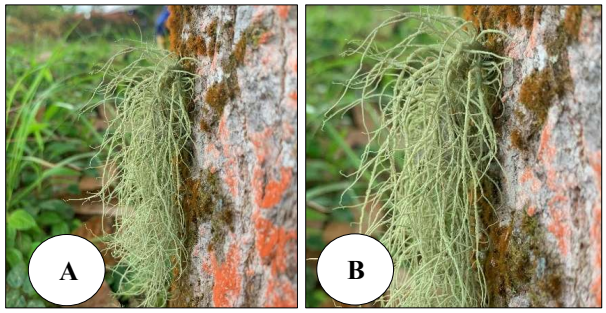

Fig. 1: Morphology of *Usnea longissima* Ach. **(**A) Thallus. (B) Dichotomous structure of thallus

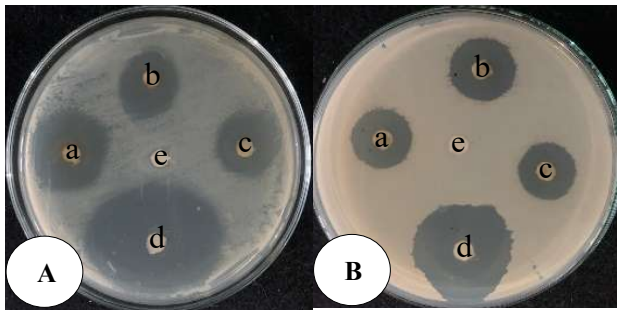

Fig. 2: U. longissima methanol extract bacteria inhibition zones: A. Gram-positive P. acnes ATCC 6919; (a–c). Replicates of methanol extract of U. longissima; d. Positive control and e. Negative control and B. Gram-negative P. aeruginosa ATCC 15442

GC-MS Analysis

Raw GC-MS data and individual chromatograms were processed using Origin software. GC-MS analysis revealed 29 bioactive compounds in *U. longissima*. These compounds include 9-octadecenal, (z)-, carbamic acid, monoammonium salt, propanedioic acid, butanoic acid, methane, sulfinylbis-, 2H-tetrazol-2-ethanal, 5-methyl-, hexanoic acid, 1,3-propanediol, 2-butyl-2-ethyl-, cyclopentanol, 3-methyl-, L-alanine, N-acetyl-, 2-pyrrolidinone, formamide, N-(2,4-dimethylphenyl)-, isosorbide, 1,4-benzenediol, 2,3,5-trimethyl-, ethanone, 1-(3-butyloxiranyl)-, undecanoic acid, 10-bromo-, 4-methoxy-2-propylphenol, 1-propanone, 1-(2,4,6-trihydroxyphenyl)-, benzoic acid, 2,4-dihydroxy-3,5,6-trimethyl-, methyl ester, benzoic acid, 2-hydroxy-4-methoxy-3,5,6-trimethyl-, methyl ester, tetradecanoic acid, hexadecanoic acid, methyl ester, benzoic acid, 2,4-dihydroxy-6-methyl-, methyl ester, hexadecanoic acid, 9,12-octadecadienoic acid (*Z,Z*)-, methyl ester, tetradecanoic acid, ethyl ester, 4N-methylamino-2(1H)-pyrimidinone, oxacycloheptadec-8-en-2-one, cyclohexane, and 1,4-dimethyl-2-octadecyl-. The retention times are listed in Table 2, and the chromatograms are shown in Fig. 3. According to PubChem screening, some compounds lacked existing 3D structures; therefore, for docking analysis, 28 of the compounds listed in the database were utilized.

Table 1: *U. longissima* methanol extracts antimicrobial properties

Extract	Pathogenic Microorganism		Diameter of inhibition zone (mm)		
			U. longissima Methanol Extract (10 µl/disk)	Chloramphenicol	Ketoconazole
U. longissima	Gram-Negative	*S. enterica* serovar Typhii IPBCC b 11 669	15.1±1,21	28.53	
		E. coli ATCC 8739	18.03±0,11	18.4	
		P. aeruginosa ATCC 15442	18.36±0,33	27	
	Gram-Positive	*S. aureus* ATCC 6538	17.16±0,10	26.06	
		P. acnes ATCC 6919	22.3±0,5	42.1	
		S. mutans ATCC 35668	18.86±0,07	37.76	
	Pathogenic Yeast	*C. albicans* ATCC 10231	9.43±0,57		31.16

Table 2: Compounds of U. longissima

No	Compound name	Mol. Formula	Mass (g/mol)	R. time (min)	Smiles	PubChem ID
1	9-octadecenal, (z)-	C18H34O	266	0.2	CCCCCCCCC=CCCCCCCCC=O	5364492
2	Carbamic acid, monoammonium salt	CH6N2O2	78	1.804	C(=O)(N)[O-].[NH4+]	517232
3	Propanedioic acid	C3H4O4	104	3.382	C(C(=O)O)C(=O)O	867
4	Butanoic acid	C4H8O2	88	6.35	CCCC(=O)O	264
5	Methane, sulfinylbis-	C2H6OS	78	8.555	CS(=O)C	679
6	2H-Tetrazol-2-ethanal, 5-methyl-	C4H6N4O	126	9.993	CC1=NN(N=N1)CC=O	535502
7	Hexanoic acid	C6H12O2	116	11.448	CCCCCC(=O)O	8892
8	1,3-Propanediol, 2-butyl-2-ethyl-	C9H20O2	160	13.039	CCCCC(CC)(CO)CO	61038
9	Cyclopentanol, 3-methyl-	C6H12O	100	14.719	CC1CCC(C1)O	86785
10	L-Alanine, N-acetyl-	C5H9NO3	131	15.691	CC(C(=O)O)NC(=O)C	88064
11	2-pyrrolidinone	C4H7NO	85	16.341	C1CC(=O)NC1	12025
12	Formamide, N-(2,4-dimethylphenyl)-	C9H11NO	149	17.405	CC1=CC(=C(C=C1)NC=O)C	92363
13	Isosorbide	C6H10O4	146	19.432	C1C(C2C(O1)C(CO2)O)O	12597
14	1,4-Benzenediol, 2,3,5-trimethyl-	C9H12O2	152	23.475	CC1=CC(=C(C(=C1O)C)C)O	12785
15	Ethanone, 1-(3-butyloxiranyl)-	C8H14O2	142	25.132	CCCCC1C(O1)C(=O)C	538285
16	Undecanoic acid, 10-bromo-	C11H21BrO2	264	26.362	C(CCCCCBr)CCCCC(=O)O	17812
17	4-Methoxy-2-propylphenol	C10H14O2	166	27.097	CCCC1=C(C=CC(=C1)OC)O	288671
18	1-Propanone, 1-(2,4,6-trihydroxyphenyl)-	C9H10O4	182	27.942	CCC(=O)C1=C(C=C(C=C1O)O)O	3362
19	Benzoic acid, 2,4-dihydroxy-3,5,6-trimethyl-, methyl ester	C11H14O4	210	29.531	CC1=C(C(=C(C(=C1C(=O)OC)O)C)O)C	591722
20	Benzoic acid, 2-hydroxy-4-methoxy-3,5,6-trimethyl-, methyl ester	C12H16O4	224	30.119	CC1=C(C(=C(C(=C1C(=O)OC)O)C)OC)C	606018
21	Tetradecanoic acid	C14H28O2	228	30.617	CCCCCCCCCCCCCC(=O)O	11005
22	Hexadecanoic acid, methyl ester	C17H34O2	270	31.372	CCCCCCCCCCCCCCCC(=O)OC	8181
23	Benzoic acid, 2,4-dihydroxy-6-methyl-, methyl ester	C9H10O4	182	32.985	CC1=CC(=CC(=C1C(=O)OC)O)O	76658
24	Hexadecanoic acid	C16H32O2	256	34.636	CCCCCCCCCCCCCCCC(=O)O	985
25	9,12-Octadecadienoic acid (Z,Z)-, methyl ester	C19H34O2	294	35.29	CCCCCC=CCC=CCCCCCCCC(=O)OC	5284421
26	Tetradecanoic acid, ethyl ester	C16H32O2	256	36.349	CCCCCCCCCCCCCC(=O)OCC	31283
27	4N-methylamino-2(1H)-pyrimidinone	C5H7N3O	125	37.412	CNC1=NC=CC(=O)N1	14803475
28	Oxacycloheptadec-8-en-2-one	C16H28O2	252	38.303	C1CCCCOC(=O)CCCCCC=CCCC1	5365703
29	Cyclohexane, 1,4-dimethyl-2-octadecyl-	C26H52	364	39.475	CCCCCCCCCCCCCCCCCCC1CC(CCC1C)C	282770

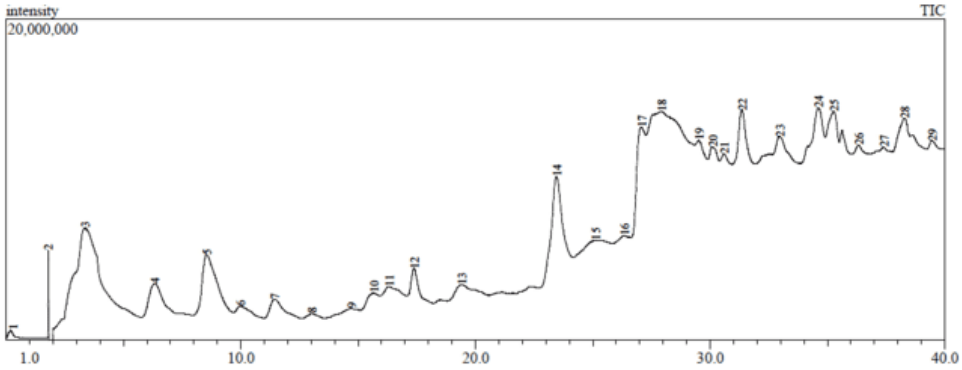

Fig. 3: Gas chromatography-mass spectrometry results for U. longissimi

Prediction of Compound Biological Activities

Numerous bioactive compounds in *U. longissima* Ach. exhibited significant potential for various biological activities, as indicated by the results of PASS online analysis (**Table 3**). One of the most prominent compounds, 9-octadecenal (*Z*)-, stands out with a high probability of activity (Pa) because it functions as a membrane integrity antagonist (Pa=0.886). This result suggests that the compound can disrupt cell membranes, making it a promising candidate for applications that target cell membrane stability. Additionally, 9-octadecenal (*Z*)- showed strong inhibitory potential against polyporopepsin (Pa=0.789), further emphasizing its potential to inhibit specific protease enzymes involved in microbial pathogenesis. Compounds such as propanedioic acid and butanoic acid also demonstrated strong inhibitory activities against a variety of pepsin-like enzymes, including saccharopepsin (Pa=0.945 for propanedioic acid and Pa=0.957 for butanoic acid) and chymosin (Pa=0.945 for propanedioic acid and Pa=0.957 for butanoic acid). These inhibitory effects on proteases suggest that these compounds are potent candidates for enzyme-targeted antimicrobial therapies, potentially affecting protein degradation processes in pathogens. In contrast, certain compounds such as methane and sulfinylbis did not show significant biological activity under the tested conditions, indicating limited or no relevance for antimicrobial or enzymatic inhibition applications. However, compounds such as cyclopentanol and 3-methyl displayed strong anti-eczematic activity (Pa=0.921) and moderate antifungal properties (Pa=0.560), making them interesting compounds for potential use in dermatological treatments.

In summary, *U. longissima* Ach. contains a wide array of biologically active compounds with notable applications, particularly in enzyme inhibition and disruption of membrane integrity. These compounds show potential for antimicrobial and enzyme-targeted therapeutic development, although some may require further optimization to enhance their efficacy across broader biological activities.

Prediction of Drug-Likeness

The compounds derived from *U. longissima* showed varying degrees of adherence to the drug-likeness requirements. Compounds such as 9-octadecenal (*Z*)- (MlogP 4.68), hexadecanoic acid methyl ester (MlogP 4.44), 9,12-octadecadienoic acid (*Z*, *Z*) methyl ester (MlogP 4.7), and tetradecanoic acid ethyl ester (MlogP 4.19) deviated from Lipinski's rules, primarily because of their elevated MlogP values, which exceeded the recommended threshold of 4.15. These high MlogP values suggest issues with permeability, which may negatively affect the drug-like properties and bioavailability. In contrast, compounds such as propanedioic acid (MlogP -0.99), butanoic acid (MlogP 0.49), and cyclopentanol, 3-methyl- (MlogP 1.14) adhered well to Lipinski's rules, with MlogP values below the threshold and acceptable hydrogen bond counts. These characteristics indicate better potential for oral bioavailability, making them more favorable candidates for drug development. Most *U. longissima* Ach. compounds also meet Lipinski's molecular weight and hydrogen bond donor/acceptor requirements, suggesting their drug-like potential. High MlogP values frequently result in high lipophilicity, which can make it hard for medicines to be absorbed, distributed, broken down, and flushed out of the body. Lipinski *et al*. (2001) suggested the "rule of five," which states that when the logP exceeds certain thresholds, poor absorption and penetration are more likely, and excessive lipophilicity may lead to inferior pharmacokinetic features. More recent research supports these findings, showing that compounds with high MlogP values commonly face difficulties in drug development and require modifications to improve their pharmacokinetic profiles and overall drug likeness (Wenlock and Barton, 2013; Bhal *et al*., 2007). These findings underscore the need to refine the molecular characteristics of therapeutic candidates to improve their efficacy and safety profiles (Arnott and Planey, 2012).

Table 3: Prediction biological activity compounds of U. longissima

No	Compound Name	Biological activity	Pa	Pi	Criteria
1	9-Octadecenal, (Z)-	Membrane integrity antagonist	0.886	0.003	High
		Polyporopepsin inhibitor	0.789	0.022	High
		Sphinganine kinase inhibitor	0.789	0.015	High
2	Carbamic acid, monoammonium salt	-	-	-	-
3	Propanedioic acid	Saccharopepsin antagonist	0.945	0.003	High
		Chymosin suppressor	0.945	0.003	High
		Acrocylindropepsin blocker	0.945	0.003	High
		Pullulanase inhibitor	0.931	0.002	High
		Dextranase inhibitor	0.925	0.002	High
4	Butanoic acid	Saccharopepsin inhibitor	0.957	0.002	High
		Acrocylindropepsin blocker	0.957	0.002	High
		Chymosin suppressor	0.957	0.002	High
5	Methane, sulfinylbis-	-	-	-	-
6	2H-Tetrazol-2-ethanal, 5-methyl-	Polyporopepsin inhibitor	0.675	0.046	Low
		Feruloyl esterase inhibitor	0.665	0.025	Low
		Inhibitor of POMC converting enzyme	0.649	0.035	Low
7	Hexanoic acid	Acrocylindropepsin blocker	0.961	0.002	High
		Saccharopepsin antagonist	0.961	0.002	High
		Chymosin suppressor	0.961	0.002	High
8	1,3-Propanediol, 2-butyl-2-ethyl-	Dextranase inhibitor	0.909	0.003	High
		Saccharopepsin antagonist	0.892	0.006	High
		Chymosin suppressor	0.892	0.006	High
9	Cyclopentanol, 3-methyl-	Antieczematic	0.921	0.004	High
		Antifungal	0.560	0.023	low
		Antiseborrheic	0.839	0.012	High
10	L-Alanine, N-acetyl-	Chymosin suppressor	0.952	0.002	High
		Acrocylindropepsin blocker	0.952	0.002	High
		Polyporopepsin inhibitor	0.939	0.003	High
		Saccharopepsin antagonist	0.952	0.002	High
11	2-Pyrrolidinone	Chloride peroxidase inhibitor	0.847	0.003	High
		Mannan endo-1,4-beta-mannosidase inhibitor	0.836	0.002	High
		Yeast ribonuclease inhibitor	0.748	0.004	High
12	Formamide, N-(2,4-dimethylphenyl)-	Glutamyl endopeptidase II inhibitor	0.766	0.015	High
		Chymosin suppressor	0.646	0.060	Low
		Saccharopepsin antagonist	0.646	0.060	Low
13	Isosorbide	Pectate Lyase Inhibitor	0.700	0.005	High
		Polyporopepsin inhibitor	0.756	0.028	High
		Manganese peroxidase inhibitor	0.789	0.005	High
14	1,4-Benzenediol, 2,3,5-trimethyl-	Antiseborrheic	0.848	0.010	High
		Antiseptic	0.807	0.004	High
		Membrane stability enhancer	0.906	0.010	High
15	Ethanone, 1-(3-butyloxiranyl)-	Acrocylindropepsin blocker	0.874	0.008	High
		Antifungal	0.517	0.028	Low
		Saccharopepsin inhibitor	0.874	0.008	High
16	Undecanoic acid, 10-bromo-	Prolyl aminopeptidase inhibitor	0.901	0.004	High
		Acrocylindropepsin blocker	0.897	0.005	High
		Saccharopepsin antagonist	0.897	0.005	High
17	4-Methoxy-2-propylphenol	Sebum-controlling	0.880	0.006	High
		Acrocylindropepsin blocker	0.822	0.016	High
		Chymosin suppressor	0.822	0.016	High
18	1-Propanone, 1-(2,4,6-trihydroxyphenyl)-	Membrane stability enhancer	0.907	0.009	High
		Antiseborrheic	0.887	0.005	High
		Saccharopepsin antagonist	0.795	0.021	High
19	Benzoic acid, 2,4-dihydroxy-3,5,6-trimethyl-, methyl ester	Membrane stability enhancer	0.905	0.010	High
		Antiinflammatory	0.817	0.005	High
		Antiseborrheic	0.825	0.014	High
20	Benzoic acid, 2-hydroxy-4-methoxy-3,5,6-trimethyl-, methyl ester	Membrane stability enhancer	0.878	0.017	High
		Antiinflammatory	0.807	0.006	High

		Membrane permeability inhibitor	0.776	0.014	High
21	Tetradecanoic acid	Acrocylindropepsin blocker	0.961	0.002	High
		Saccharopepsin inhibitor	0.961	0.002	High
		Inhibitor of glucan endo-1,3-beta-D-glucosidase	0.945	0.002	High
22	Hexadecanoic acid, methyl ester	Saccharopepsin antagonist	0.962	0.002	High
		Acrocylindropepsin blocker	0.942	0.003	High
		Chymosin suppressor	0.962	0.002	High
		Acylcarnitine hydrolase inhibitor	0.942	0.003	High
23	Benzoic acid, 2,4-dihydroxy-6-methyl-, methyl ester	Membrane stability enhancer	0.927	0.005	High
		Antiseptic	0.802	0.004	High
		Antiseborrheic	0.881	0.006	High
24	Hexadecanoic acid	Saccharopepsin antagonist	0.961	0.002	High
		Chymosin suppressor	0.961	0.002	High
		CYP2J substrate	0.962	0.002	High
		Acrocylindropepsin blocker	0.961	0.002	High
25	9,12-Octadecadienoic acid (Z,Z)-, methyl ester	Antieczematic	0.953	0.002	High
		Antifungal	0.507	0.029	Low
		Saccharopepsin antagonist	0.936	0.003	High
26	Tetradecanoic acid, ethyl ester	Cutinase blocker	0.946	0.001	High
		Saccharopepsin antagonist	0.919	0.004	High
		Chymosin suppressor	0.919	0.004	High
27	4N-methylamino-2(1H)-pyrimidinone	Chloride peroxidase inhibitor	0.847	0.003	High
		Pterin deaminase inhibitor	0.804	0.004	High
		Chenodeoxycholoyltaurine hydrolase inhibitor	0.650	0.012	Low
28	Oxacycloheptadec-8-en-2-one	Acrocylindropepsin blocker	0.801	0.020	High
		Chymosin suppressor	0.801	0.020	High
		Saccharopepsin antagonist	0.801	0.020	High

Molecular Interactions of Bioactive Compounds U. longissima *Ach. with 6KZZ*

The control substances were compared based on the molecular docking modeling results. 4-[[8-(Methylamino)-2-oxidanylidene-1~{H}-quinolin-3-yl[carbonylamino]benzoic acid9 and several bioactive compounds from *U. longissima* showed substantial differences in the type of interaction and binding energy to protein targets. 4-[[8-(Methylamino)-2-oxidanylidene-1~{H}-quinolin-3-yl[carbonylamino]benzoic acid9, as a control compound, exhibited the highest binding energy of all chemicals examined at −6.2 kcal/mol. The major contacts are hydrogen bonds with residues His55, Asp74, Arg136, Glu137, and Thr163 and hydrophobic interactions with residues Lys57 and Arg76; this interaction demonstrates its high affinity for the target. 4-[[8-(Methylamino)-2-oxidanylidene-1~{H}-quinolin-3-yl[carbonylamino]benzoic acid9 efficiently inhibited the target protein (Table 4).

Twenty-eight bioactive compounds isolated from *U. longissima* Ach. demonstrated diverse binding potentials for DNA gyrase in molecular docking studies, highlighting its potential for antimicrobial applications. Among these compounds, 1-propanone, 1-(2,4,6-trihydroxyphenyl)- exhibited the highest binding energy (−4.8 kcal/mol) (Table 5). It forms hydrogen bonds with Glu50 and Arg76 and hydrophobic interactions with Ala53, which are further supported by electrostatic interactions with Asp49. These results suggest strong interactions and potential biological activity. In contrast, the control compound, 4-[[8-(methylamino)-2-oxidanylidene-1~{H}-quinolin-3-yl[carbonylamino]benzoic acid, showed a binding affinity of −6.2 kcal/mol, interacting via hydrogen bonds with residues such as His55, Asp74, Arg136, and Glu137, as well as hydrophobic interactions with Thr163. Its stronger binding affinity indicates higher potential for biological effectiveness than those of most *U. longissima* compounds. Some compounds, such as benzoic acid, 2,4-dihydroxy-3,5,6-trimethyl-, methyl ester (−5.0 kcal/mol), and oxacycloheptadec-8-en-2-one (−5.1 kcal/mol), showed notable binding affinities. Benzoic acid interacts with Arg76 through hydrogen bonds, indicating promising bioactivity, whereas oxacycloheptadec-8-en-2-one shows significant hydrophobic interactions, indicating potential antimicrobial activity.

In contrast, compounds such as 9-octadecenal, (*Z*)- (−3.6 kcal/mol) and carbamic acid, monoammonium salt (−2.8 kcal/mol) showed lower binding energies, forming limited hydrophobic interactions and weaker hydrogen bonds. These lower affinities suggest that these compounds have weaker biological effects and require further optimization to enhance their efficacy. In summary, although several compounds from *U. longissima* showed promising interactions with DNA gyrase, a few displayed weak binding affinities, indicating the need for structural modifications to improve their bioactivity and interaction strength.

Table 4: Physicochemical properties of compounds from *U. longissima*

No	Compound Name	Lipinski				
		MW	**MlogP ≤ 4.15**	**NorO ≤ 10**	**NHorOH ≤ 5**	**Violasi**
1	9-Octadecenal, (Z)-	266	4.68	1	0	Yes (1)
2	Carbamic acid, monoammonium salt	78	-6.14	2	2	Yes (0)
3	Propanedioic acid	104	-0.99	4	2	Yes (0)
4	Butanoic acid	88	0.49	2	1	Yes (0)
5	Methane, sulfinylbis-	78	-0.37	1	0	Yes (0)
6	2H-Tetrazol-2-ethanal, 5-methyl-	126	-0.69	4	0	Yes (0)
7	Hexanoic acid	116	1.27	2	1	Yes (0)
8	1,3-Propanediol, 2-butyl-2-ethyl-	160	1.61	2	2	Yes (0)
9	Cyclopentanol, 3-methyl-	100	1.14	1	1	Yes (0)
10	L-Alanine, N-acetyl-	131	-0.54	3	2	Yes (0)
11	2-Pyrrolidinone	85	-0.31	1	1	Yes (0)
12	Formamide, N-(2,4-dimethylphenyl)-	149	2.25	1	1	Yes (0)
13	Isosorbide	146	-1.52	4	2	Yes (0)
14	1,4-Benzenediol, 2,3,5-trimethyl-	152	1.8	2	2	Yes (0)
15	Ethanone, 1-(3-butyloxiranyl)-	142	0.76	2	0	Yes (0)
16	Undecanoic acid, 10-bromo-	264	3.29	2	1	Yes (0)
17	4-Methoxy-2-propylphenol	166	2.1	2	1	Yes (0)
18	1-Propanone, 1-(2,4,6-trihydroxyphenyl)-	182	0.24	4	2	Yes (0)
19	Benzoic acid, 2,4-dihydroxy-3,5,6-trimethyl-, methyl ester	210	1.65	4	2	Yes (0)
20	Benzoic acid, 2-hydroxy-4-methoxy-3,5,6-trimethyl-, methyl ester	224	1.93	4	1	Yes (0)
21	Tetradecanoic acid	228	3.69	2	1	Yes (0)
22	Hexadecanoic acid, methyl ester	270	4.44	2	0	Yes (1)
23	Benzoic acid, 2,4-dihydroxy-6-methyl-, methyl ester	182	1.06	4	2	Yes (0)
24	Hexadecanoic acid	256	4.19	2	1	Yes (1)
25	9,12-Octadecadienoic acid (Z,Z)-, methyl ester	294	4.7	2	0	Yes (1)
26	Tetradecanoic acid, ethyl ester	256	4.19	2	0	Yes (1)
27	4N-methylamino-2(1H)-pyrimidinone	125	-0.44	2	2	Yes (0)
28	Oxacycloheptadec-8-en-2-one	252	3.69	2	0	Yes (0)

Table 5: Residue and biding energy of ligand and 6KZZ interaction

No	Ligands	Interaction Type					Binding Afinity
		Hydrogen Bond		Hydrophobic	Electrostatis	Unfavorable	
		Hydrogen Bond	Carbon Hydrogen Bond				
Control							
1	4-[[8-(methylamino)-2-oxidanylidene-1~{H}-quinolin-3-yl]carbonylamino]benzoic acid9 (Control)	HIS 55, ASP 74, ARG 136, GLU 137	THR 163	LYS 57, ARG 76			-6.2
Bioactive components of the *U. longissima*							
1	9-Octadecenal, (Z)-			ALA 53, ILE 94			-3.6
2	Carbamic acid, monoammonium salt	GLN 135, THR 163	GLY 164			GLN 72	-2.8
3	Propanedioic acid	ASN 46, GLU 50					-3.5
4	Butanoic acid	THR 62, SER 70		ILE 62			-3.2
5	Methane, sulfinylbis-	THR 62, SER 70					-2.1
6	2H-Tetrazol-2-ethanal, 5-methyl-	THR 62, SER 70, ARG 206		ILE 60			-4
7	Hexanoic acid	GLN 135	GLY 164	LYS 162			-3.6

8	1,3-Propanediol, 2-butyl-2-ethyl-	ASP 73, GLN 135		ILE 60, LYS 162		GLN 72	-3.9
9	Cyclopentanol, 3-methyl-						-3.7
10	L-Alanine, N-acetyl-	THR 62		ILE 60			-3.9
11	2-Pyrrolidinone	GLU 50		ALA 53			-3.2
12	Formamide, N-(2,4-dimethylphenyl)-				ASP 49, GLU 50		-4.3
13	Isosorbide	THR 62, SER 70					-4
14	1,4-Benzenediol, 2,3,5-trimethyl-	GLU 50					-4.6
15	Ethanone, 1-(3-butyloxiranyl)-	ARG 76	ASP 49				-3.6
16	Undecanoic acid, 10-bromo-	ARG 204		ILE 60			-4
17	4-Methoxy-2-propylphenol	GLU 50		ALA 53, ILE 94	ASP 49		-4.4
18	1-Propanone, 1-(2,4,6-trihydroxyphenyl)-	GLU 50, ARG 76		ALA 53	ASP 49		-4.8
19	Benzoic acid, 2,4-dihydroxy-3,5,6-trimethyl-, methyl ester	ARG 76					-5
20	Benzoic acid, 2-hydroxy-4-methoxy-3,5,6-trimethyl-, methyl ester	SER 70, ARG 206	THR 62	ILE 60, MET 166, LYS 208			-4.5
21	Tetradecanoic acid	ILE 60, THR 62, SER 70					-3.8
22	Hexadecanoic acid, methyl ester	THR 62, SER 70		ILE 60, HIS 64, LYS 162			-4
23	Benzoic acid, 2,4-dihydroxy-6-methyl-, methyl ester	GLU 50, ARG 76		ALA 53	ASP 49		-4.9
24	Hexadecanoic acid	SER 202, ARG 204		ILE 60, LYS 162			-4
25	9,12-Octadecadienoic acid (Z,Z)-, methyl ester	THR 62, SER 70		ILE 60, HIS 64, LYS 162			-4.2
26	Tetradecanoic acid, ethyl ester	ARG 204		ILE 60, LYS 162			-3.9
27	4N-methylamino-2(1H)-pyrimidinone	THR 62, SER 70		ILE 60, MET 166			-4
28	Oxacycloheptadec-8-en-2-one						-5.1

Discussion

In Vitro Evaluation of Bioactive Compounds from U. longissima

U. longissima methanol extract shows promise against pathogens. The largest inhibition zone was observed against *P. acnes* ATCC 6919 (22.3 ± 0.5 mm), indicating strong effects against Gram-positive bacteria and suggesting that this extract may disrupt cell wall synthesis more effectively in these organisms. For Gram-negative bacteria, the largest inhibition zone was recorded against *P. aeruginosa* ATCC 15442 (18.36 ± 0.33 mm), indicating good penetration capabilities. Furthermore, against C. albicans ATCC 10231, the methanolic extract showed modest antifungal activity, with an inhibition zone of 9.43 ± 0.57 mm. Although this value is lower than its antibacterial activity, it suggests potential antifungal properties. These findings underscore the broad-spectrum antimicrobial potential of the *U. longissima* methanol extract, particularly against Gram-positive bacteria, and highlight the need for further investigation into its active compounds and their mechanisms of action.

Gram-positive bacteria lack an outer membrane and have a durable, porous peptidoglycan layer. This structural simplicity allows antimicrobial agents, including antimicrobial peptides, to penetrate and reach the cytoplasmic membrane more easily, where they exert their antimicrobial effects. In contrast, gram-negative bacteria have a more complicated cell envelope with lipopolysaccharide in the external membrane. The outer membrane acts as an additional barrier, preventing many antimicrobial agents from accessing the inner cell structures. The negative charge of the outer membrane creates electrostatic repulsion, which reduces the penetration ability of cationic antimicrobial peptides (Hancock, 1997). Furthermore, gram-negative bacteria often possess efflux pumps and other resistance mechanisms, which further decrease the effectiveness of antimicrobial agents (Hui-Wen and Francis, 2007). Because their membranes are more complicated and they have more defences, gram-negative bacteria are harder for

antibiotics to kill. The membrane composition, particularly the presence of lipopolysaccharides, strongly influences how antimicrobial peptides interact with and disrupt bacterial membranes (Epand *et al*., 2016).

In Silico Evaluation of Bioactive Compounds from *U. longissima*

Molecular docking studies with DNA gyrase (6KZZ) demonstrated that various bioactive components of *U. longissima* Ach. exhibited potential antimicrobial activity. The 3D and 2D interactions between the ligands and DNA gyrase (6KZZ) are shown in **Fig. 4** and **Fig. 5**. The control compound, 4-[[8-(methylamino)-2-oxidanylidene-1~{H}-quinolin-3-yl]carbonylamino]benzoic acid9, strongly bound with key residues His55, Asp74, Arg136, and Glu137, along with hydrophobic interactions involving Thr163. This binding resulted in a binding affinity of −6.2 kcal/mol, indicating its high potential for inhibiting microbial targets. Among the bioactive compounds from *U. longissima*, benzoic acid, 2,4-dihydroxy-3,5,6-trimethyl-, and methyl ester demonstrated notable binding energy (−5.0 kcal/mol) by hydrogen bonding to Arg76, suggesting that they may exhibit comparable inhibitory effects against microbial targets. Another promising compound, oxacycloheptadec-8-en-2-one, also showed strong binding affinity (−5.1 kcal/mol), indicating potential biological activity.

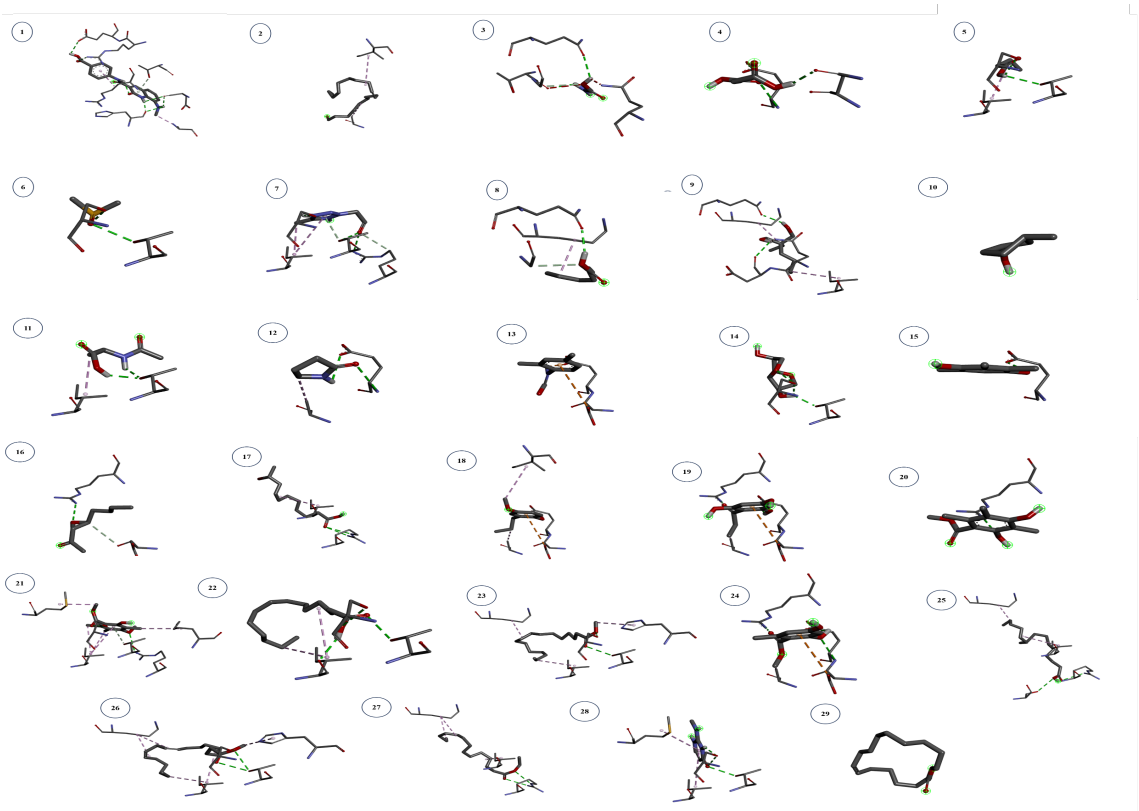

Fig. 4: 3D interactions of 2-{1-[2-amino-2-(4-hydroxy-phenyl)-acetylamino]-2-oxo-ethyl}-5,5-dimethyl-thiazolidine-4-carboxylic acid (control) and bioactive compounds from U. longissima Ach. against 6KZZ protein. (1) 4-[[8-(methylamino)-2-oxidanylidene-1~{H}-quinolin-3-yl]carbonylamino]benzoic acid9, (2) 9-octadecenal, (z)-, (3) carbamic acid, monoammonium salt, (4) propanedioic acid, (5) butanoic acid, (6) methane, sulfinylbis-, (7) 2H-tetrazol-2-ethanal, 5-methyl-, (8) hexanoic acid, (9) 1,3-propanediol, 2-butyl-2-ethyl-, (10) cyclopentanol, 3-methyl-, (11) L-alanine, N-acetyl-, (12) 2-pyrrolidinone, (13) formamide, N-(2,4-dimethylphenyl)-, (14) isosorbide, (15) 1,4-benzenediol, 2,3,5-trimethyl-, (16) ethanone, 1-(3-butyloxiranyl)-, (17) undecanoic acid, 10-bromo-, (18) 4-methoxy-2-propylphenol, (19) 1-propanone, 1-(2,4,6-trihydroxyphenyl)-, (20) benzoic acid, 2,4-dihydroxy-3,5,6-trimethyl-, methyl ester, (21) benzoic acid, 2-hydroxy-4-methoxy-3,5,6-trimethyl-, methyl ester, (22) tetradecanoic acid, (23) hexadecanoic acid, methyl ester, (24) benzoic acid, 2,4-dihydroxy-6-methyl-, methyl ester, (25) hexadecanoic acid, (26) 9,12-octadecadienoic acid (Z,Z)-, methyl ester, (27) tetradecanoic acid, ethyl ester, (28) 4N-methylamino-2(1H)-pyrimidinone, and (29) oxacycloheptadec-8-en-2-one.

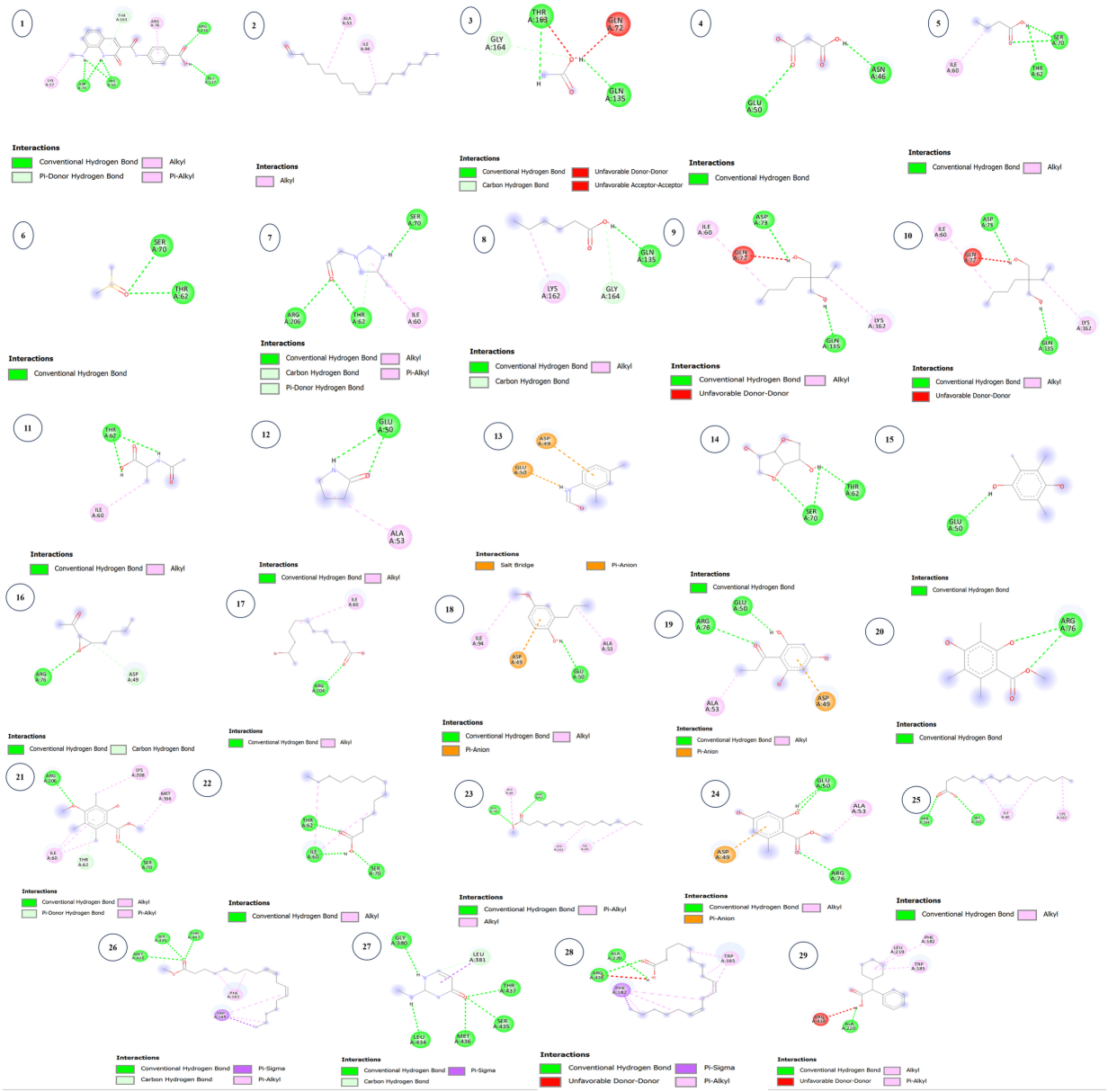

Fig. 5: 2D interactions of 2-{1-[2-amino-2-(4-hydroxy-phenyl)-acetylamino]-2-oxo-ethyl}-5,5-dimethyl-thiazolidine-4-carboxylic acid (control) and bioactive compounds from U. longissima Ach. against the 6KZZ protein. (1) 4-[[8-(methylamino)-2-oxidanylidene-1~{H}-quinolin-3-yl]carbonylamino]benzoic acid9, (2) 9-octadecenal, (z)-, (3) carbamic acid, monoammonium salt, (4) propanedioic acid, (5) butanoic acid, (6) methane, sulfinylbis-, (7) 2H-tetrazol-2-ethanal, 5-methyl-, (8) hexanoic acid, (9) 1,3-propanediol, 2-butyl-2-ethyl-, (10) cyclopentanol, 3-methyl-, (11) L-alanine, N-acetyl-, (12) 2-pyrrolidinone, (13) formamide, N-(2,4-dimethylphenyl)-, (14) isosorbide, (15) 1,4-benzenediol, 2,3,5-trimethyl-, (16) ethanone, 1-(3-butyloxiranyl)-, (17) undecanoic acid, 10-bromo-, (18) 4-methoxy-2-propylphenol, (19) 1-propanone, 1-(2,4,6-trihydroxyphenyl)-, (20) benzoic acid, 2,4-dihydroxy-3,5,6-trimethyl-, methyl ester, (21) benzoic acid, 2-hydroxy-4-methoxy-3,5,6-trimethyl-, methyl ester, (22) tetradecanoic acid, (23) hexadecanoic acid, methyl ester, (24) benzoic acid, 2,4-dihydroxy-6-methyl-, methyl ester, (25) hexadecanoic acid, (26) 9,12-octadecadienoic acid (Z,Z)-, methyl ester, (27) tetradecanoic acid, ethyl ester, (28) 4N-methylamino-2(1H)-pyrimidinone, and (29) oxacycloheptadec-8-en-2-one

Furthermore, by establishing hydrogen bonds with Glu50 and ARG 76 and hydrophobic contacts with Ala53, 1-propanone, 1-(2,4,6-trihydroxyphenyl)- demonstrated a considerable binding energy of −4.8 kcal/mol. These interactions suggest that the compound can interfere with microbial cell processes, making it a viable candidate for antimicrobial development. However, some compounds demonstrated weaker binding affinities, such as 9-

octadecenal, (*Z*)- (−3.6 kcal/mol), which interacts only through hydrophobic interactions with Ala53 and Ile94. In the same way, carbamic acid, a monoammonium salt, bonded to Gln135 and Thr163 by hydrogen bonding and had a reduced binding energy of -2.8 kcal/mol. These weaker interactions suggest that these compounds have less potent antimicrobial effects and require further optimization. In conclusion, several bioactive compounds from U. longissima exhibited promising binding affinities and interactions with key residues of DNA gyrase, suggesting their potential as antimicrobial agents. The development of novel therapies against microbial pathogens may be facilitated by further investigation of these compounds, particularly those with increased binding energies.

DNA gyrase B from E. coli is an essential enzyme in bacterial DNA replication, transcription, and repair and is responsible for introducing negative supercoils into DNA to relieve tension during strand unwinding. DNA gyrase B plays a critical role in the ATP-dependent strand passage mechanism, and inhibitors that target this subunit can block its activity by binding to the ATP-binding domain, preventing ATP hydrolysis, and thus disrupting the supercoiling process. This interference with DNA replication makes DNA gyrase B a valuable target for antimicrobial therapies, particularly for the development of drugs aimed at combating resistant bacterial strains (Ushiyama *et al*., 2020).

Conclusion

Usnea longissima Ach. exhibits notable antimicrobial potential, with its methanol extract exhibited significant suppression against *P. acnes* (22.3±0.5 mm) and gram-negative bacteria like *P. aeruginosa* (18.36±0.33 mm). We identified 29 bioactive compounds with various biological activities, including 9-octadecenal and benzoic acid derivatives. Compounds such as 1-propanone, 1-(2,4,6-trihydroxyphenyl)-(−4.8 kcal/mol), and oxacycloheptadec-8-en-2-one (−5.1 kcal/mol) showed high binding affinities with DNA gyrase from *E. coli*, indicating their potential as antimicrobial agents. However, compounds including 9-octadecenal (−3.6 kcal/mol) and carbamic acid (−2.8 kcal/mol) showed weaker binding, suggesting the need for further optimization. Overall, *U. longissima* is a valuable resource for the development of novel antimicrobial therapies.

Acknowledgement

Gratitude is extended to Universitas Sumatera Utara for providing funding for this work under the World Class University (WCU) research program for the 2023/2024 period. This research is included in the first author's dissertation as part of the PMDSU program.

Funding Information

This study received funding from Universitas Sumatera Utara via the World Class University (WCU) research program for the 2023/2024 period.

Author's Contributions

Erman Munir: Conceptualized the study, and conceived and designed the analysis.
Oky Kusuma Atni: Collected the data and drafted the manuscript.
Nursahara Pasaribu: Contributed to data collection, performed the analysis, and participated in manuscript writing.
Etti Sartina Siregar: Edited and refined the final draft of the manuscript.
Mohd Nazre Saleh: Proofread the manuscript and contributed to writing.

Ethics

There is no new info in this study. The associated author makes sure that the work was read and accepted by all writers and that there are no ethical problems.

References

Arnott, J. A., & Planey, S. L. (2012). The Influence of Lipophilicity in Drug Discovery and Design. *Expert Opinion on Drug Discovery*, *7*(10), 863–875. https://doi.org/10.1517/17460441.2012.714363

Atni, O. K., Munir, E., Siregar, E. S., & Saleh, M. N. (2024). Lichen Diversity and Taxonomy in Bukit Barisan Grand Forest Park, North Sumatra, Indonesia. *Biodiversitas Journal of Biological Diversity*, *25*(4), 1623–1630. https://doi.org/10.13057/biodiv/d250431

Badiali, C., Petruccelli, V., Brasili, E., & Pasqua, G. (2023). Xanthones: Biosynthesis and Trafficking in Plants, Fungi and Lichens. *Plants*, *12*(4), 694. https://doi.org/10.3390/plants12040694

Bhal, S. K., Kassam, K., Peirson, I. G., & Pearl, G. M. (2007). The Rule of Five Revisited: Applying Log D in Place of Log P in Drug-Likeness Filters. *Molecular Pharmaceutics*, *4*(4), 556–560. https://doi.org/10.1021/mp0700209

Bhattarai, H. D., Kim, T., Oh, H., & Yim, J. H. (2013). A New Pseudodepsidone from the Antarctic Lichen Stereocaulon Alpinum and its Antioxidant, Antibacterial Activity. *The Journal of Antibiotics*, *66*(9), 559–561. https://doi.org/10.1038/ja.2013.41

Calcott, M. J., Ackerley, D. F., Knight, A., Keyzers, R. A., & Owen, J. G. (2018). Secondary Metabolism in the Lichen Symbiosis. *Chemical Society Reviews*, *47*(5), 1730–1760. https://doi.org/10.1039/c7cs00431a

Epand, R. M., Walker, C., Epand, R. F., & Magarvey, N. A. (2016). Molecular Mechanisms of Membrane Targeting Antibiotics. *Biochimica et Biophysica Acta (BBA) - Biomembranes*, *1858*(5), 980–987. https://doi.org/10.1016/j.bbamem.2015.10.018

Gasulla, F., del Campo, E. M., Casano, L. M., & Guéra, A. (2021). Advances in Understanding of Desiccation Tolerance of Lichens and Lichen-Forming Algae. *Plants*, *10*(4), 807. https://doi.org/10.3390/plants10040807

Hancock, R. E. W. (1997). Peptide Antibiotics. *The Lancet*, *349*(9049), 418–422. https://doi.org/10.1016/s0140-6736(97)80051-7

Hui-Wen, L., & Francis, A.-O. (2007). Genetic polymorphism and function of glutathione S-transferases in tumor drug resistance. *Current Opinion in Pharmacology*, *7*(4), 367–374. https://doi.org/10.1016/j.coph.2007.06.009

Jannah, M., A`yun, Q., Afifah, N., Prasetya, E., & Hariri, M. R. (2022). Usnea in West Java: A Potential Source of Bioactive Secondary Metabolites. *Berkala Penelitian Hayati*, *28*(1), 26–31. https://doi.org/10.23869/bphjbr.28.1.20224

Johansson, O., Olofsson, J., Giesler, R., & Palmqvist, K. (2011). Lichen Responses to Nitrogen and Phosphorus Additions can be Explained by the Different Symbiont Responses. *New Phytologist*, *191*(3), 795–805. https://doi.org/10.1111/j.1469-8137.2011.03739.x

Kalra, R., Conlan, X. A., & Goel, M. (2023). Recent Advances in Research for Potential Utilization of Unexplored Lichen Metabolites. *Biotechnology Advances*, *62*, 108072. https://doi.org/10.1016/j.biotechadv.2022.108072

Lipinski, C. A., Lombardo, F., Dominy, B. W., & Feeney, P. J. (2001). Experimental and Computational Approaches to Estimate Solubility and Permeability in Drug Discovery and Development Settings. *Advanced Drug Delivery Reviews*, *46*(1–3), 3–26. https://doi.org/10.1016/s0169-409x(00)00129-0

Lücking, R., Hodkinson, B. P., & Leavitt, S. D. (2017). The 2016 Classification of Lichenized Fungi in the Ascomycota and Basidiomycota – Approaching One Thousand Genera. *The Bryologist*, *119*(4), 361–416. https://doi.org/10.1639/0007-2745-119.4.361

Macedo, D. C. S., Almeida, F. J. F., Wanderley, M. S. O., Ferraz, M. S., Santos, N. P. S., López, A. M. Q., Santos-Magalhães, N. S., & Lira-Nogueira, M. C. B. (2021). Usnic Acid: From an Ancient Lichen Derivative to Promising Biological and Nanotechnology Applications. *Phytochemistry Reviews*, *20*(3), 609–630. https://doi.org/10.1007/s11101-020-09717-1

Maulidiyah, M., Akhmad, D., Usman, U., Andi, M., La Ode, A. S., & Muhammad, N. (2021). Antioxidant Activity of Secondary Metabolite Compounds from Lichen Teloschistes flavicans. *Biointerface Research in Applied Chemistry*, *11*(6), 13878–13884. https://doi.org/10.33263/briac116.1387813884

McClendon, A. K., & Osheroff, N. (2007). DNA Topoisomerase II, Genotoxicity and Cancer. *Mutation Research/Fundamental and Molecular Mechanisms of Mutagenesis*, *623*(1–2), 83–97. https://doi.org/10.1016/j.mrfmmm.2007.06.009

Mendili, M., Khadhri, A., Mediouni-Ben Jemâa, J., Andolfi, A., Tufano, I., Aschi-Smiti, S., & DellaGreca, M. (2022). Anti-Inflammatory Potential of Compounds Isolated from Tunisian Lichens Species. *Chemistry and Biodiversity*, *19*(8), e202200134. https://doi.org/10.1002/cbdv.202200134

Mitrović, T., Stamenković, S., Cvetković, V., Tošić, S., Stanković, M., Radojević, I., Stefanović, O., Čomić, L., Đačić, D., Ćurčić, M., & Marković, S. (2011). Antioxidant, Antimicrobial and Antiproliferative Activities of Five Lichen Species. *International Journal of Molecular Sciences*, *12*(8), 5428–5448. https://doi.org/10.3390/ijms12085428

Nguyen, T. T., Yoon, S., Yang, Y., Lee, H.-B., Oh, S., Jeong, M.-H., Kim, J.-J., Yee, S.-T., Crişan, F., Moon, C., Lee, K. Y., Kim, K. K., Hur, J.-S., & Kim, H. (2014). Lichen Secondary Metabolites in Flavocetraria cucullata Exhibit Anti-Cancer Effects on Human Cancer Cells through the Induction of Apoptosis and Suppression of Tumorigenic Potentials. *PLoS ONE*, *9*(10), e111575. https://doi.org/10.1371/journal.pone.0111575

Ozturk, S., Erkisa, M., Oran, S., Ulukaya, E., Celikler, S., & Ari, F. (2021). Lichens Exerts an Anti-Proliferative Effect on Human Breast and Lung Cancer Cells Through Induction of Apoptosis. *Drug and Chemical Toxicology*, *44*(3), 259–267. https://doi.org/10.1080/01480545.2019.1573825

Dandapat, M., & Paul, S. (2019). Secondary Metabolites from Lichen Usnea Longissima and its Pharmacological Relevance. *Pharmacognosy Research*, *11*(2), 103–109. https://doi.org/10.4103/pr.pr_111_18

Ranković, B., & Kosanić, M. (2021). Biotechnological Substances in Lichens. *Natural Bioactive Compounds*, 249–265. https://doi.org/10.1016/b978-0-12-820655-3.00012-4

Suharno, Linus, Y. C., Puguh, S., & Rosye, H. R. T. (2020). Rapid Assessment of Lichen Diversity in Baliem Valley, Jayawijaya, Papua, Indonesia. *Biodiversitas Journal of Biological Diversity*, *21*(6), 2403–2409. https://doi.org/10.13057/biodiv/d210610

Tatipamula, Vinay, B., & Vamsi, K. (2021). Dibenzofurans from Cladonia Corniculata Ahti and Kashiw Inhibit Key Enzymes Involved in Inflammation and Gout: An in Vitro Approach. *Indian Journal of Chemistry -Section B*, *60*(5), 715–719. https://doi.org/10.56042/ijcb.v60i5.38966

Ushiyama, F., Amada, H., Takeuchi, T., Tanaka-Yamamoto, N., Kanazawa, H., Nakano, K., Mima, M., Masuko, A., Takata, I., Hitaka, K., Iwamoto, K., Sugiyama, H., & Ohtake, N. (2020). Lead Identification of 8-(Methylamino)-2-oxo-1,2-Dihydroquinoline Derivatives as DNA Gyrase Inhibitors: Hit-to-Lead Generation Involving Thermodynamic Evaluation. *ACS Omega*, *5*(17), 10145–10159. https://doi.org/10.1021/acsomega.0c00865

Wenlock, M. C., & Barton, P. (2013). In Silico Physicochemical Parameter Predictions. *Molecular Pharmaceutics*, *10*(4), 1224–1235. https://doi.org/10.1021/mp300537k

Yahr, R., Vildalys, R., & Depriest, P. T. (2004). Strong Fungal Specificity and Selectivity for Algal Symbionts in Florida Scrub Cladonia Lichens. *Molecular Ecology*, *13*(11), 3367–3378. https://doiorg/10.1111/j.1365-294x.2004.02350.x

Yahr, R., Vilgalys, R., & Depriest, P. T. (2006). Geographic Variation in Algal Partners of Cladonia Subtenuis (Cladoniaceae) Highlights the Dynamic Nature of a Lichen Symbiosis. *New Phytologist*, *171*(4), 847–860. https://doi.org/10.1111/j.1469-8137.2006.01792.x

Yasmin, F., & Jabin, R. (2024). Physiology of Lichen. *Chemistry, Biology and Pharmacology of Lichen*, 71–80. https://doi.org/10.1002/9781394190706.ch6